Investigation on Damping Capability of Indigenous Wood Species in Ethiopia

Fasikaw Kibrete[1] and Hailu Shimels[2(✉)]

[1] Department of Mechanical Engineering, University of Gondar, Gondar, Ethiopia
[2] Department of Mechanical Engineering, Bahir Dar Institute of Technology, Bahir Dar University, Bahir Dar, Ethiopia

Abstract. Damping capacity is a measure of a material's ability which absorb vibration energy by converting into heat energy. Materials which have high damping ability can suppress excessive vibrations to a reasonable limit. Therefore, this paper investigates the damping characteristics of five indigenous wood species (*Cordia Africana, Juniperus Procera, Afrocarpus Gracilior, Syzygium Guineense* and *Acacia Decurrens*) found in Ethiopia through analytical, numerical and experimental approaches. The experimental testing was performed using piezoelectric accelerometer in association with LabVIEW for a perfectly clamped-free cantilever beam based on the impact hammer excitation. The damping ratio was computed using logarithmic decrement method from the decay curve measured. Based on the investigation, the damping factor for all species of woods was almost equal to 0.020 at room condition, and it is definitely greater than most other crystalline materials. Thus, wooden materials are better suitable for engineering applications in terms of vibrations if the other strength properties are satisfactory.

Keywords: Damping capacity · Logarithmic decrement · Natural frequency · Vibration · Wood

1 Introduction

Vibrational motion is a repetitive type motion of the bodies with a defined time interval. The main causes of vibrational motion are unbalanced centrifugal forces, elastic nature of system, external excitations, misalignment and dry friction between contact surfaces [1]. Some vibrational motions are important with a desired amplitude and frequency for musical instruments, geological investigations, drilling of geotechnical wells and harvesting crops, but most vibrations are unwanted in many engineering applications since it results wastage of energy, high stresses, unwanted noise, rapid wear and catastrophic failure due to its excessiveness [2]. Hence, it needs to be dampened. Therefore, the interest of many researchers lies in dampening excessive vibrations using vibration damping materials [3]. These materials have high energy dissipation capability, and play a significant role in reducing noise, vibration and dynamic stresses of the mechanical and structural systems, and in prolonging its lifetime under cyclic loading or impact [4, 5].

M. A. Delele et al. (Eds.): ICAST 2020, LNICST 385, pp. 326–340, 2021.
https://doi.org/10.1007/978-3-030-80618-7_22

Damping capacity is the ability of a material's ability to absorb mechanical energy by converting it into heat during mechanical vibration [6]. It can be expressed using several parameters, including specific damping capacity, amplification factor, inverse quality factor, loss factor and logarithmic decrement. Based on their damping capacity, materials can be categorized as low damping or high damping materials. Low damping materials have higher amplitude of vibration and are required for increasing sensitivity in sensors and certain precision instrumentation, and for proper functioning as in the case with parts of musical instruments, tuning fork and bells. On the other hand, high damping materials are very desirable to suppress mechanical vibration, noise and transmission of waves. These materials are used in many engineering components like turbine buckets, propeller blades, crankshafts, automotive bumper or in other devices where a component can resonate at some frequency to minimize the resonant amplitude, and thus minimizes the dynamic stresses to which the component is exposed [7, 8].

Particularly, woods have been put forward as a high damping material due to its composite polymeric nature consisting of crystalline cellulosic microfibrils embedded in a more or less amorphous matrix [9]. The cellular network converts mechanical energy into heat by frictional and viscoelastic resistance. Because of the high internal friction created by the cellular pore network, wooden materials are advantageous for many engineering applications to exhibit adequate damping ability so that any excessive vibration is dampened to an acceptable limit in practice [10, 11].

Even if wood has numerous engineering applications and Ethiopia has plenty of higher plant species, it is not used as a standardized engineering material probably because of lack of substantial work which describes the physical and mechanical properties of every species. Particularly, the damping capacity are not studied, known and documented by the researchers, forest products processors and different stakeholders still now because of the complexity of damping determination methods, less concern and limited knowledge [12, 13]. Therefore, it becomes relevant to conduct research on the damping properties of *Cordia Africana (Wanza), Juniperus Procera (Tsid), Afrocarpus Gracilior (Zigba), Syzygium Guineense (Dokma)* and *Acacia Decurrens (Girar*).

2 Analytical Analysis for Free Transverse Vibration of Cantilever Beam

Transverse vibrations of cantilevered beams have been the subject of numerous studies based on different beam theories [14–16]. Of existing beam theories, Euler-Bernoulli beam theory is used in this investigation because the lateral dimensions of the beam are less than one-tenth of its length. This theory assumes that the rotation of the differential element is negligible compared to translation and the angular distortion due to shear is small in relation to bending deformation [17].

2.1 Free Transverse Vibration Analysis of Cantilever Beam Without Damping

Figure 1 shows a cantilever beam which undergoes free vibration with the transverse displacement of $y(x, t)$.

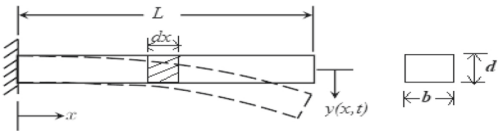

Fig. 1. Cantilever beam under free vibration.

The beam vibration is governed by partial differential equations in terms of spatial variable x and time variable t. Thus, the governing equations of motion for the free transverse vibration for Euler-Bernoulli beam is given by [18];

$$\frac{\mathrm{EI}}{\rho \mathrm{A}} \frac{\partial^4 \mathrm{y}(\mathrm{x}, \mathrm{t})}{\partial \mathrm{x}^4} + \frac{\partial^2 \mathrm{y}(\mathrm{x}, \mathrm{t})}{\partial \mathrm{x}^2} = 0 \tag{1}$$

where E is the Young's Modulus, ρ is the mass density of beam material, $I = bd^3/12$ is the second moment of inertia of the beam, $A = bd$ is the cross-sectional area of the beam, and b and d are the width and depth of the beam cross-section, respectively.

For uniform beam, i.e. EI is constant, Eq. (1) can be reduced to;

$$\mathrm{C}^2 \frac{\partial^4 \mathrm{y}(\mathrm{x}, \mathrm{t})}{\partial \mathrm{x}^4} + \frac{\partial^2 \mathrm{y}(\mathrm{x}, \mathrm{t})}{\partial \mathrm{x}^2} = 0 \tag{2}$$

where $\mathrm{C} = \sqrt{EI/\rho A}$ is a constant.

The governing equation is solved using the method of separation of variables, and the transverse displacement response $y(x, t)$ is written as a function of position and time as;

$$\mathrm{y}(\mathrm{x}, \mathrm{t}) = \mathrm{W}(\mathrm{x})\mathrm{T}(\mathrm{t}) \tag{3}$$

where W(x) is the space function which is described as;

$$\mathrm{W}(\mathrm{x}) = \mathrm{C}_1 \cosh\, \beta\mathrm{x} + \mathrm{C}_2\, \sinh\, \beta\mathrm{x} + \mathrm{C}_3\, \cos\, \beta\mathrm{x} + \mathrm{C}_4 \sin\, \beta\mathrm{x} \tag{4}$$

and T(t) is the time-dependent amplitude described as;

$$\mathrm{T}(\mathrm{t}) = \mathrm{B}_1\, \sin\, \omega t + \mathrm{B}_2\, \cos\, \omega t \tag{5}$$

where $\beta = \sqrt[4]{\frac{\rho \mathrm{A} \omega^2}{\mathrm{C}^2}}$ is a constant, $\omega = \beta^2 \sqrt{\frac{EI}{\rho A}}$ is the is the circular natural frequency, B_1 and B_2 are constants evaluated from the initial conditions; and real constants C_i are evaluated om the boundary conditions of the beam. Therefore, the transverse deflection of the cantilever beam at the free end is calculated as;

$$\mathrm{y}(\mathrm{x}, \mathrm{t}) = W(x) * \left[\frac{\mathrm{y_o}}{\mathrm{W(L)}} \cos\, \omega_\mathrm{n} \mathrm{t} \right] \tag{6}$$

where $\mathrm{W}(\mathrm{x}) = \frac{(\cosh\, \beta\mathrm{x} - \cos\, \beta\mathrm{x})(\sin\, \beta\mathrm{x} + \sinh\, \beta x) + (\sinh\, \beta\mathrm{x} - \sin\, \beta x)(\cos\, \beta x + \cosh\, \beta x)}{(\cos\, \beta x + \cosh\, \beta x)}$, and ω_n is the natural frequency of the beam.

It is fact that continuous systems have an infinite degree of freedom. Therefore, an infinite number of natural frequencies of the cantilever beam are given by;

$$\omega_i = (\beta_i L)^2 \sqrt{\frac{EI}{\rho A l^4}} \tag{7}$$

where the values of $\beta_i l$ are 1.875104, 4.69409 and 7.85475 for the first three consecutive modes. Based on Eq. (7), the natural frequencies of a vibrating body depend on its geometry and material properties, and its determination is of vital importance for predicting resonant damages.

2.2 Free Transverse Vibration Analysis of Cantilever Beam with Damping

The governing equation of free transverse vibration of cantilever beam has been deeply investigated by many researchers, in particular, to take into account the effect of damping on the dynamic behavior of the beam. Even a large amount of literature is available on the subject of damping, there is no any single well-established empirical formula which represents the damping of the beam. Therefore, for a cantilever beam undergoing small deformation, linear beam theory is used for a given excitation. Based on the theory, the behavior of the first mode of vibration can be approximated to the behavior of a single degree of freedom spring mass damper system (see Fig. 2).

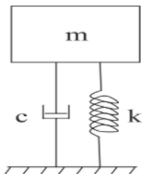

Fig. 2. Spring mass damper system for single degree of freedom.

With these assumptions, the vibration of such a linear system is described by the popular equation as;

$$\ddot{x} + 2\zeta\omega_1\dot{x} + \omega_1^2 x = 0 \tag{8}$$

where ω_1 is the fundamental natural frequency, ζ is the damping factor, and $x, \dot{x}$ and $\ddot{x}$ are the system response in terms of displacement, velocity and acceleration, respectively.

The fundamental natural frequency ω_1 is given by;

$$\omega_1 = \sqrt{k/m} \tag{9}$$

The damping value at the first natural frequency of each sample is quantified using an equivalent damping factor which is obtained from the time history graph using the logarithmic decrement method. It correlates damping with the fundamental natural frequency and the mass of the beam. Thus, the damping factor is given by;

$$\zeta = \frac{c}{2\sqrt{km}} = \frac{c}{2m\omega_1} \tag{10}$$

where k is the stiffness, c is the damping coefficient, and m is the mass.
Therefore, the general solution to the equation is obtained as follows;

$$x(t) = A.e^{-\zeta\omega_1 t}\cos(\omega_d.t + \phi) \tag{11}$$

where A is the amplitude of vibration determined from initial conditions, ϕ is a phase angle that depends on the initial velocity, and ω_d represent the damped natural frequencies of the system for the first mode. Therefore, the undamped and damped natural frequencies are related to each other as;

$$\omega_d = \omega_1\sqrt{1-\zeta^2} \tag{12}$$

If the tip of the cantilever beam is driven to an initial displacement and then left free to oscillate, the vibration is analytically obtained for the following initial conditions: $x(0) = x_0$ and $x_0 = 0$. In this case, the value of the vibration amplitude is calculated as;

$$A = \frac{x_0}{\sqrt{1-\zeta^2}} \tag{13}$$

and the phase angle can be

$$\phi = \tan^{-1}\left(\frac{-\zeta}{\sqrt{1-\zeta^2}}\right) \tag{14}$$

3 Numerical Analysis for Free Transverse Vibration of Cantilever Beam

There are numerous numerical methods which are used for the free transverse vibration analysis of cantilever beam due to advancement in computational techniques and availability of software. Out of many, finite element analysis is an efficient numerical tool to solve problems of continuous systems [19]. In this paper, the numerical analysis is carried out using ANSYS software.

3.1 Numerical Analysis Without Damping

Many practical problems encountered in engineering applications are mathematically modeled by differential equations. In most problems, it is difficult to get an accurate solution. Thus, an approximate solution is applied to solve such problems. Therefore, the finite element method based on the Galerkin's method of residual approach is used in this study. This approach is a most popular and powerful method for finding approximate solutions of differential equations by transforming into an appropriate integral equation [20, 21].

By applying the Galerkin's method, therefore, the governing equations of motion of the free transverse vibration stated in Eq. (1) is modified as [22];

$$\int_0^L \left(\frac{EI}{\rho A}\frac{\partial^4 y(x,t)}{\partial x^4} + \frac{\partial^2 y(x,t)}{\partial x^2}\right) w dx = 0 \tag{15}$$

where L is the beam length and $w(x)$ is the Galerkin's weighting function.
For n number of elements of length l, Eq. (15) can be modified as;

$$\sum_{i=1}^{n}\left[\int_0^l \rho\, A\frac{\partial^2 y}{\partial x^2}w\,dx + \int_0^l EI\frac{\partial^2 y}{\partial x^2}\frac{\partial^2 w}{\partial x^2}dx\right] = 0 \tag{16}$$

Therefore, Eq. (16) can be modified as;

$$\sum_{i=1}^{n}\left([m]\{\ddot{d}\} + [k]\{d\}\right) = 0 \tag{17}$$

where {d} represents the nodal displacements, {d"} denotes the second derivative of nodal displacement with time at the nodes. The mass [m] and stiffness [k] matrices are given by;

$$[m] = \rho\, A\int_0^1 [N]^T[N]\;dx = \frac{\rho\, A}{420}\begin{bmatrix} 156 & 22l & 54 & -13l \\ 22l & 4l^2 & 13l & -3l^2 \\ 54 & 13l & 156 & -22l \\ -13l & -3l^2 & -22l & 4l^2 \end{bmatrix} \tag{18}$$

and,

$$[k] = EI\int_0^l \left[\ddot{N}\right]^T\left[\ddot{N}\right]dx = \frac{EI}{l^3}\begin{bmatrix} 12 & 6l & -12 & 6l \\ 6l & 4l^2 & -6l & 2l^2 \\ -12 & -6l & 12 & -6l \\ 6l & 2l^2 & -6l & 4l^2 \end{bmatrix} \tag{19}$$

By considering the effect of all the elements, Eq. (17) is further modified to;

$$[M]\left\{\ddot{D}\right\} + [K]\{D\} = 0 \tag{20}$$

where [M] and [K] are the system mass and stiffness matrices and, $\{D\}$ and $\left\{\ddot{D}\right\}$ are the displacement and acceleration vectors of all the nodes of the entire beam, respectively. This equation represents the equation of motion for the free undamped vibration and its solution is given by;

$$\{D\} = \{\phi\}e^{i\omega t} \tag{21}$$

where ω and ϕ are the natural frequency (eigenvalue) and mode shapes (eigenvector) of vibration, respectively.
Substituting Eq. (21) into Eq. (20) and it results;

$$\left[[K] - \omega^2[M]\right]\{\phi\} = 0 \tag{22}$$

The solutions of Eq. (22) give the natural frequencies of the system. The positive values of ω is the first lowest frequency called fundamental natural frequency.

3.2 Numerical Analysis with Damping

In the above derivations, the effect of damping is not considered since the direct formation of the damping matrix is very difficult in actual practice. But in ANSYS there are different ways which introduce the effect of damping, each of them being suitable for a particular case. In this investigation, therefore, the damping matrix [c] is determined by using Rayleigh damping theory in which the damping matrix is a function of mass [m] and stiffness [k] matrices that can be linearized with α and β as constants. The damping matrix can be determined as [23];

$$[c] = \alpha[m] + \beta[k] \tag{23}$$

where α and β are the Rayleigh damping coefficients which can be determined from specified experimental damping factor. In many practical cases, the resonance frequencies are relatively high. Therefore, the damping component related to the mass (the term involving α) is negligible. In such case, the β damping from i^{th} mode can be evaluated from known values of ζ_i and ω_i which represents material damping. Thus;

$$\zeta_i = \frac{\beta\omega_i}{2} \tag{24}$$

For the first natural frequency of the cantilever beam, the damping factor can be calculated as;

$$\zeta = \frac{\beta\omega_1}{2} = 1.758\ \beta\sqrt{\frac{EI}{\rho Al^4}} \tag{25}$$

3.3 Natural Frequencies and Mode Shapes Using Numerical Method

In order to prove the correctness of the results obtained from the analytical analysis in terms of the spacing between natural frequencies, a finite element model of the beam mounted in a cantilever configuration was developed using ANSYS APDL. In the pre-processor of the main menu, the beam 2 node 188 element was selected to perform the numerical analysis using ANSYS APDL on to which the boundary conditions for cantilever are imposed. The Young's modulus, density and Poisson's ratio values of the materials were given as input parameters. Using modeling option, the beam was generated as 2D entity of the beam. In meshing tool option, the beam was uniformly meshed into 10 equal parts and each element had 2 nodes (i.e., a total of 11 nodes in the system). It was assumed that 2 DOFs per node (translation along y-axis and rotation about z-axis), therefore the DOFs of each element were 4 and the DOFs of the system are 22. Therefore, the size of both element stiffness and mass matrices were (4x4), and the size of system stiffness and mass matrices were (22x22). In this work, Block Lanczos mode-extraction methods is used since it is preferable for large symmetric problems, and has fast convergence. The number of modes to extract and expand was equal to five. Finally, the results were obtained from General Post Processor.

Using Eq. (18) and (19), therefore, the size of the system stiffness and system mass matrices can be expressed as;

System stiffness matrix, [K] =

$$\frac{EI}{l^3}*\begin{bmatrix}
12 & 6l & -12 & 6l & 0 & 0 & 0 & 0 & 0 & 0 & 0 & 0 & 0 & 0 & 0 & 0 & 0 & 0 & 0 & 0 & 0 & 0 \\
6l & 4l^2 & -6l & 2l^2 & 0 & 0 & 0 & 0 & 0 & 0 & 0 & 0 & 0 & 0 & 0 & 0 & 0 & 0 & 0 & 0 & 0 & 0 \\
-12 & -6l & 24 & 0 & -12 & 6l & 0 & 0 & 0 & 0 & 0 & 0 & 0 & 0 & 0 & 0 & 0 & 0 & 0 & 0 & 0 & 0 \\
6l & 2l^2 & 0 & 8l^2 & -6l & 2l^2 & 0 & 0 & 0 & 0 & 0 & 0 & 0 & 0 & 0 & 0 & 0 & 0 & 0 & 0 & 0 & 0 \\
0 & 0 & -12 & -6l & 24 & 0 & -12 & 6l & 0 & 0 & 0 & 0 & 0 & 0 & 0 & 0 & 0 & 0 & 0 & 0 & 0 & 0 \\
0 & 0 & 6l & 2l^2 & 0 & 8l^2 & -6l & 2l^2 & 0 & 0 & 0 & 0 & 0 & 0 & 0 & 0 & 0 & 0 & 0 & 0 & 0 & 0 \\
0 & 0 & 0 & 0 & -12 & -6l & 24 & 0 & -12 & 6l & 0 & 0 & 0 & 0 & 0 & 0 & 0 & 0 & 0 & 0 & 0 & 0 \\
0 & 0 & 0 & 0 & 6l & 2l^2 & 0 & 8l^2 & -6l & 2l^2 & 0 & 0 & 0 & 0 & 0 & 0 & 0 & 0 & 0 & 0 & 0 & 0 \\
0 & 0 & 0 & 0 & 0 & 0 & -12 & -6l & 24 & 0 & -12 & 6l & 0 & 0 & 0 & 0 & 0 & 0 & 0 & 0 & 0 & 0 \\
0 & 0 & 0 & 0 & 0 & 0 & 6l & 2l^2 & 0 & 8l^2 & -6l & 2l^2 & 0 & 0 & 0 & 0 & 0 & 0 & 0 & 0 & 0 & 0 \\
0 & 0 & 0 & 0 & 0 & 0 & 0 & 0 & -12 & -6l & 24 & 0 & -12 & 6l & 0 & 0 & 0 & 0 & 0 & 0 & 0 & 0 \\
0 & 0 & 0 & 0 & 0 & 0 & 0 & 0 & 6l & 2l^2 & 0 & 8l^2 & -6l & 2l^2 & 0 & 0 & 0 & 0 & 0 & 0 & 0 & 0 \\
0 & 0 & 0 & 0 & 0 & 0 & 0 & 0 & 0 & 0 & -12 & -6l & 24 & 0 & -12 & 6l & 0 & 0 & 0 & 0 & 0 & 0 \\
0 & 0 & 0 & 0 & 0 & 0 & 0 & 0 & 0 & 0 & 6l & 2l^2 & 0 & 8l^2 & -6l & 2l^2 & 0 & 0 & 0 & 0 & 0 & 0 \\
0 & 0 & 0 & 0 & 0 & 0 & 0 & 0 & 0 & 0 & 0 & 0 & -12 & -6l & 24 & 0 & -12 & 6l & 0 & 0 & 0 & 0 \\
0 & 0 & 0 & 0 & 0 & 0 & 0 & 0 & 0 & 0 & 0 & 0 & 6l & 2l^2 & 0 & 8l^2 & -6l & 2l^2 & 0 & 0 & 0 & 0 \\
0 & 0 & 0 & 0 & 0 & 0 & 0 & 0 & 0 & 0 & 0 & 0 & 0 & 0 & -12 & -6l & 24 & 0 & -12 & 6l & 0 & 0 \\
0 & 0 & 0 & 0 & 0 & 0 & 0 & 0 & 0 & 0 & 0 & 0 & 0 & 0 & 6l & 2l^2 & 0 & 8l^2 & -6l & 2l^2 & 0 & 0 \\
0 & 0 & 0 & 0 & 0 & 0 & 0 & 0 & 0 & 0 & 0 & 0 & 0 & 0 & 0 & 0 & -12 & -6l & 24 & 0 & -12 & 6l \\
0 & 0 & 0 & 0 & 0 & 0 & 0 & 0 & 0 & 0 & 0 & 0 & 0 & 0 & 0 & 0 & 6l & 2l^2 & 0 & 8l^2 & -6l & 2l^2 \\
0 & 0 & 0 & 0 & 0 & 0 & 0 & 0 & 0 & 0 & 0 & 0 & 0 & 0 & 0 & 0 & 0 & 0 & -12 & -6l & 12 & -6l \\
0 & 0 & 0 & 0 & 0 & 0 & 0 & 0 & 0 & 0 & 0 & 0 & 0 & 0 & 0 & 0 & 0 & 0 & 6l & 2l^2 & -6l & 4l^2
\end{bmatrix}$$

System mass matrix, [M] =

$$\frac{\rho A}{420}*\begin{bmatrix}
156 & 22l & 54 & -13l & 0 & 0 & 0 & 0 & 0 & 0 & 0 & 0 & 0 & 0 & 0 & 0 & 0 & 0 & 0 & 0 & 0 & 0 \\
22l & 4l^2 & 13l & -3l^2 & 0 & 0 & 0 & 0 & 0 & 0 & 0 & 0 & 0 & 0 & 0 & 0 & 0 & 0 & 0 & 0 & 0 & 0 \\
54 & 13l & 312 & 0 & 54 & -13l & 0 & 0 & 0 & 0 & 0 & 0 & 0 & 0 & 0 & 0 & 0 & 0 & 0 & 0 & 0 & 0 \\
-13l & -3l^2 & 0 & 8l^2 & 13l & -3l^2 & 0 & 0 & 0 & 0 & 0 & 0 & 0 & 0 & 0 & 0 & 0 & 0 & 0 & 0 & 0 & 0 \\
0 & 0 & 54 & 13l & 312 & 0 & 54 & -13l & 0 & 0 & 0 & 0 & 0 & 0 & 0 & 0 & 0 & 0 & 0 & 0 & 0 & 0 \\
0 & 0 & -13l & -3l^2 & 0 & 8l^2 & 13l & -3l^2 & 0 & 0 & 0 & 0 & 0 & 0 & 0 & 0 & 0 & 0 & 0 & 0 & 0 & 0 \\
0 & 0 & 0 & 0 & 54 & 13l & 312 & 0 & 54 & -13l & 0 & 0 & 0 & 0 & 0 & 0 & 0 & 0 & 0 & 0 & 0 & 0 \\
0 & 0 & 0 & 0 & -13l & -3l^2 & 0 & 8l^2 & 13l & -3l^2 & 0 & 0 & 0 & 0 & 0 & 0 & 0 & 0 & 0 & 0 & 0 & 0 \\
0 & 0 & 0 & 0 & 0 & 0 & 54 & 13l & 312 & 0 & 54 & -13l & 0 & 0 & 0 & 0 & 0 & 0 & 0 & 0 & 0 & 0 \\
0 & 0 & 0 & 0 & 0 & 0 & -13l & -3l^2 & 0 & 8l^2 & 13l & -3l^2 & 0 & 0 & 0 & 0 & 0 & 0 & 0 & 0 & 0 & 0 \\
0 & 0 & 0 & 0 & 0 & 0 & 0 & 0 & 54 & 13l & 312 & 0 & 54 & -13l & 0 & 0 & 0 & 0 & 0 & 0 & 0 & 0 \\
0 & 0 & 0 & 0 & 0 & 0 & 0 & 0 & -13l & -3l^2 & 0 & 8l^2 & 13l & -3l^2 & 0 & 0 & 0 & 0 & 0 & 0 & 0 & 0 \\
0 & 0 & 0 & 0 & 0 & 0 & 0 & 0 & 0 & 0 & 54 & 13l & 312 & 0 & 54 & -13l & 0 & 0 & 0 & 0 & 0 & 0 \\
0 & 0 & 0 & 0 & 0 & 0 & 0 & 0 & 0 & 0 & -13l & -3l^2 & 0 & 8l^2 & 13l & -3l^2 & 0 & 0 & 0 & 0 & 0 & 0 \\
0 & 0 & 0 & 0 & 0 & 0 & 0 & 0 & 0 & 0 & 0 & 0 & 54 & 13l & 312 & 0 & 54 & -13l & 0 & 0 & 0 & 0 \\
0 & 0 & 0 & 0 & 0 & 0 & 0 & 0 & 0 & 0 & 0 & 0 & -13l & -3l^2 & 0 & 8l^2 & 13l & -3l^2 & 0 & 0 & 0 & 0 \\
0 & 0 & 0 & 0 & 0 & 0 & 0 & 0 & 0 & 0 & 0 & 0 & 0 & 0 & 54 & 13l & 312 & 0 & 54 & -13l & 0 & 0 \\
0 & 0 & 0 & 0 & 0 & 0 & 0 & 0 & 0 & 0 & 0 & 0 & 0 & 0 & -13l & -3l^2 & 0 & 8l^2 & 13l & -3l^2 & 0 & 0 \\
0 & 0 & 0 & 0 & 0 & 0 & 0 & 0 & 0 & 0 & 0 & 0 & 0 & 0 & 0 & 0 & 54 & 13l & 312 & 0 & 54 & -13l \\
0 & 0 & 0 & 0 & 0 & 0 & 0 & 0 & 0 & 0 & 0 & 0 & 0 & 0 & 0 & 0 & -13l & -3l^2 & 0 & 8l^2 & 13l & -3l^2 \\
0 & 0 & 0 & 0 & 0 & 0 & 0 & 0 & 0 & 0 & 0 & 0 & 0 & 0 & 0 & 0 & 0 & 0 & 54 & 13l & 156 & -22l \\
0 & 0 & 0 & 0 & 0 & 0 & 0 & 0 & 0 & 0 & 0 & 0 & 0 & 0 & 0 & 0 & 0 & 0 & -13l & -3l^2 & -22l & 4l^2
\end{bmatrix}$$

The system stiffness and mass matrices are used to find out the eigenvalues and eigenvectors of the vibration. The eigenvalues and eigenvectors can be real or complex depending on the damping value. However, the damping effect is generally neglected in the determination of eigenvalues and eigenvectors of a lightly vibrating system. Therefore, real eigenvalues and eigenvectors are derived from the assumed equation of motion

of undamped vibration. This assumption fairly holds good in most of the practical cases where damping is less pronounced.

4 Experimental Analysis

In both analytical and numerical approaches, the starting three natural frequencies were calculated, and there was also a need to determine the damping ratio. But it is impossible because of no empirical formula for assessing damping. Therefore, experimental analysis was established for the determination of damping ratio using logarithmic decrement method from the time response graph.

4.1 Materials, Specimen Preparations and Physical Conditions

Five species of woods such as *Cordia Africana (Wanza), Juniperus Procera (Tsid), Afrocarpus Gracilior (Zigba), Syzygium Guineense (Dokma) and Acacia Decurrens (Girar)* were selected to perform the experimentation. These species of woods were collected around Bahir Dar and their age were estimated as above 30 years. The material properties of these wood under at 12% moisture content are tabulated in Table 1.

Table 1. Material properties of the selected wood species [12, 13].

Species	Density (kg/m^3)	Young's modulus (N/mm^2)	Poisson's ratio
Cordia Africana	410	6996	0.39
Juniperus Procera	540	9081	0.47
Afrocarpus Gracilior	520	6704	0.45
Syzygium Guineense	740	11229	0.43
Acacia Decurrens	816	14310	0.46

For this experiment, five specimens of each species were prepared along the grain with a dimension of 240 × 12 × 3 mm^3 based on ASTM E-756 vibrating beam technique. Based on the standard, uniform cantilever beam configuration having a specimen dimension of 240 × 12 × 3 mm^3 were selected for all wood species because it is a simple, fast, cost efficient and time saving technique [24–26].

After preparation, all the specimens were first dried in order to reach equilibrium in adsorption. Since the oven-drying method is the most universally accepted method for determining moisture content, drying was performed for 48 h in an oven dry set at 60 °C to prevent cracking of specimens [27, 28]. Then, the samples were conditioned at a temperature of 20 ± 2 °C and a relative humidity of 65 ± 5% until experimentation.

4.2 Experimental Set-Up

The experimental set-up for the free transverse vibration testing of the selected wood materials was shown in Fig. 3.

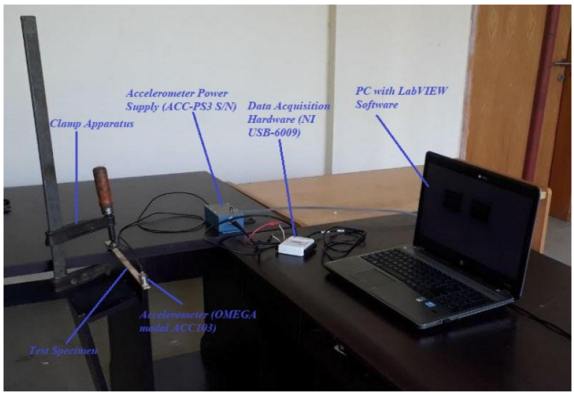

Fig. 3. Experimental set-up for the cantilever beam vibration testing.

The accelerometer (OMEGA modal ACC103) is attached with a cantilever beam at the free end and connected to NI data acquisition (NI USB-6009) to acquire, store and analyze vibration data received from sensor using LabVIEW.

Figure 4 and Fig. 5 shows the block diagram and front panel of the main LabVIEW program to measure the exponentially decay curves and the natural frequencies. Before running the program, the voltage sensitivity of ACC103 accelerometer was given as an input which is equal to 0.001019 $\frac{volt}{m/s^2}$.

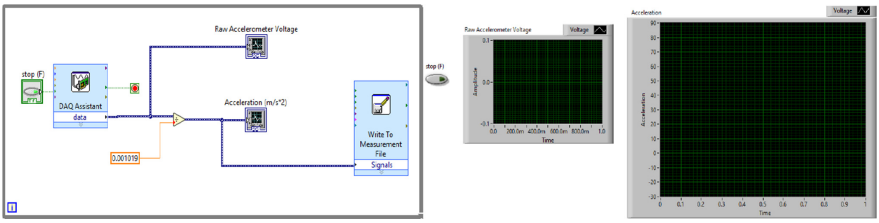

Fig. 4. LabVIEW block diagram and front panel for showing time domain.

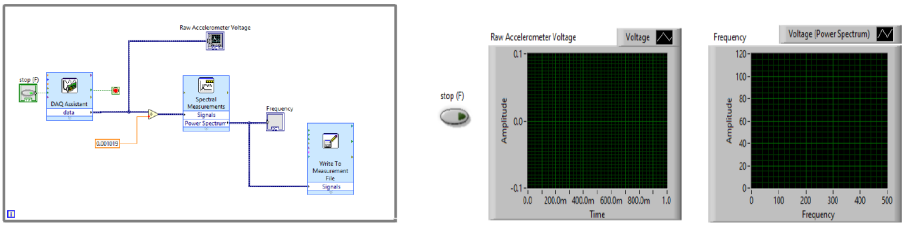

Fig. 5. LabVIEW block diagram and front panel for showing frequency domain.

4.3 Experimental Procedures

After specimen preparation, the specimen was fixed with a clamp at one end and free at the other. In order to take the measurements, the specimens were disturbed initially using impact hammer. The piezoelectric accelerometer connected to a LabVIEW program attached at the free end of the specimen sense data and generate a signal by the data acquisition device. Finally, the computer displays the required plots. The plots are subsequently used to evaluate of logarithmic decrement, damping factor and natural frequency of all the specimens from the time history curve.

Based on the decay graph, the logarithmic decrement (δ) can be estimated using the expression;

$$\delta = \frac{1}{n}.ln\left(\frac{X_1}{X_{n+1}}\right) \tag{26}$$

where x_1, x_{n+1} and n are the first cycle amplitude, last cycle amplitude and the number of cycles, respectively. Since the logarithmic decrement is more accurate with the increasing number of cycles n, the peak amplitudes in this investigation are obtained for six decrements i.e., $n = 6$ [29, 30].

Based on the calculated logarithmic decrement, the damping factor (ζ) is analyzed as;

$$\zeta = \frac{\delta}{\sqrt{4\pi^2 + \delta^2}} \tag{27}$$

The fundamental natural frequency is read directly from the data recorded with the aid of accelerometer associated with the desired LabVIEW block diagram.

5 Result and Discussion

5.1 Analytical and Numerical Natural Frequencies

The analytical and numerical natural frequencies of the selected wood materials at the first three modes of vibration are tabulated in Table 2.

The first mode is bending mode of vibration where beam tends to bend about the root sections. The second mode of vibration is bending mode where the natural frequency is greater than initial mode of vibration. The third mode shape shows the first twisting mode which has the highest frequency in all the above mode shapes.

Table 2. Comparison of analytical and numerical natural frequencies at the first three modes.

Species	Modes	Analytical Natural Frequency (Hz)	Numerical Natural Frequency (Hz)
Cordia Africana	1	34.754	34.788
	2	217.803	222.37
	3	609.854	648.51
Juniperus Procera	1	34.502	34.525
	2	216.222	220.72
	3	605.428	643.51
Afrocarpus Gracilior	1	30.209	30.229
	2	189.320	193.27
	3	530.10	563.52
Syzygium Guineense	1	32.774	32.796
	2	205.393	209.69
	3	575.106	611.44
Acacia Decurrens	1	35.233	35.256
	2	220.803	225.40
	3	618.255	657.19

5.2 Experimental Damping Factor and Natural Frequency

From the acceleration vs time plots the damping factor is analyzed using the logarithmic decrement method. Therefore, the value of the damping factor of all the selected wood species materials is shown in Table 3.

Table 3. Experimental damping factor.

Species	Damping Factor
Cordia Africana	0.020
Juniperus Procera	0.019
Afrocarpus Gracilior	0.019
Syzygium Guineense	0.020
Acacia Decurrens	0.020

Based on the amplitude vs frequency graphs, the fundamental natural frequency of the selected wooden materials at a given dimension is shown in Table 4.

Table 4. Experimental fundamental natural frequency.

Species	Fundamental Natural Frequency (Hz)
Cordia Africana	35.2
Juniperus Procera	35.8
Afrocarpus Gracilior	33
Syzygium Guineense	33.8
Acacia Decurrens	40.2

Therefore, the analytical and numerical natural frequency of the selected woods at the first mode of vibration are tabulated with the experimental results as shown in Table 5.

Table 5. Comparison of fundamental natural frequencies.

Species	Analytical Fundamental Natural Frequency (Hz)	Numerical Fundamental Natural Frequency (Hz)	Experimental Fundamental Natural Frequency (Hz)
Cordia Africana	34.754	34.788	35.2
Juniperus Procera	34.502	34.525	35.8
Afrocarpus Gracilior	30.209	30.229	33
Syzygium Guineense	32.774	32.796	33.8
Acacia Decurrens	35.233	35.256	40.2

6 Conclusions

In this paper, the analytical and numerical analysis of a cantilever beam of five different wood species materials were studied upon for finding out the first three natural frequencies. The analyses assumed the Euler-Bernoulli beam theory by considering the beam model as a discrete system. There was also a need for analytical and numerical damping estimation, but it was impossible because of no empirical formula. Therefore, the experimental testing was performed using piezoelectric accelerometer in association with LabVIEW for a perfectly clamped-free cantilever beam based on the impact hammer excitation. The damping ratio was computed by using logarithmic decrement method. The experimental testing also verifies the natural frequencies obtained theoretically at the first mode of vibration. Therefore, the following conclusions are drawn on the basis of result.

- The natural frequencies as determined by the analytical and numerical methods has almost good agreement. But the experimentally measured fundamental natural frequency shows slight variation with the theoretically calculated. The variation is caused due to the assumptions made in both analytical and numerical analysis.
- By comparing the obtained natural frequencies of five wood species, it is seen that *Acacia Decurrens* recorded the highest natural frequency while *Afrocarpus Gracilior* recorded the lowest for the same cross section and length.
- The average value of damping factor for the selected wood species with a given dimension is almost equal to 0.020 at room temperature. This is definitely greater than for most other crystalline materials like metals and its alloys. Thus, woods are better suited for mechanical and structural applications subjected to vibrations if the other strength properties are satisfactory.

7 Future Work

In the present investigation, the free vibrational characteristics and damping properties of five species of wood materials were conducted by considering the sample as a cantilever beam for mathematical simplicity. The influence of moisture content and density on material damping were only considered. Therefore, it will be interesting to dig deeper into the following issues for further investigations.

1. The present analysis can be extended for forced vibration conditions and different beam configurations.
2. The investigation can be extended for several wood species with the increased number of specimens.
3. It can also be extended by considering various parameters affecting the damping capacity of materials.

References

1. Anekar, N.: Design and testing of unbalanced mass mechanical vibration exciter. Int. J. Res. Eng. Technol. **3**(8), 107–112 (2014)
2. Visnapuu, A.: Damping Properties of Selected Steels and Cast Irons (1987)
3. Chung, D.: Review: materials for vibration damping. J. Mater. Sci. **36**(24), 5733–5737 (2001)
4. Hui, L., Xianping, W., Tao, Z., Zhijun, C., Qianfeng, F.: Design, fabrication, and properties of high damping metal matrix composites-a review. Materials **2**, 958–977 (2009)
5. Orban, F.: Damping of materials and members in structures. J. Phys. Conf. Ser. **268**(1), 1–15 (2011)
6. Sawant, H.: Experimental verification of damping coefficient by half power band width method. Int. J. Res. Aeronaut. Mech. Eng. **2**(7), 8–13 (2014)
7. Zhang, J., Perez, R.J., Lavernia, E.J.: Documentation of damping capacity of metallic, ceramic and metal-matrix composite materials. J. Mater. Sci. **28**(9), 2395–2404 (1993). https://doi.org/10.1007/BF01151671
8. Leite, E., Souza, T., Rabelo, G.: Estimation of the dynamic elastic properties of wood from Copaifera langsdorffii Desf using resonance analysis. Cerne **18**(1), 41–47 (2012)

9. Mclean, J., Arnould, O., Beauchêne, J., Clair, B.: The viscoelastic properties of some Guianese woods. In: Plant Biomechanics Conference – Cayenne, pp. 498–504 (2009)
10. Owal, D., Sanap, B.: Experimental investigation of damping performance of viscoelastic materials. Int. J. Curr. Eng. Technol. **5**, 18–21 (2016)
11. Ashby, M.F., Shercliff, H., Cebon, D.: Materials Engineering, Science, Processing and Design. 1st edn. Elsevier Ltd., University of Cambridge, UK (2007)
12. Desalegn, A., Demel, T., Gezahegn, A.: Commercial Timber Species in Ethiopia: Characteristics and Uses - A Handbook for Forest Industries, Construction and Energy Sectors, Foresters and Other Stakeholders. Addis Ababa University Press, Addis Ababa (2012)
13. Mamo, K.: Vegetative Propagation of Selected Indigenous Trees of Ethiopia (2002)
14. Gawande, H.: Investigations on effect of notch on performance evaluation of cantilever beams. Int. J. Acoust. Vib. **22**(4), 493–500 (2017)
15. Rezaee, M., Fekrmandi, H.: A theoretical and experimental investigation on free vibration vehavior of a cantilever beam with a breathing crack. Shock Vib. **19**(2), 175–186 (2012)
16. Duan, Y., Wang, J., Liu, Y., Shao, F.: Theoretical and experimental study on the transverse vibration properties of an axially moving nested cantilever beam. J. Sound Vib. **333**(13), 2885–2897 (2014)
17. Harris, M., Piersol, G.: Shock and Vibration Handbook. 5th edn. McGrawHill, New York, USA (2002)
18. Romaszko, M., Sapiński, B., Sioma, A.: Forced vibrations analysis of a cantilever beam using the vision method. J. Theor. Appl. Mech. **53**(1), 243–254 (2015)
19. Tripathy, K., Mishra, K., Mohanty, S.: Model analysis of variation of taper angle for cantilever and simply supported beam. IJIRSET **4**(11), 11353–11360 (2015)
20. Jafari, M., Djojodihardjo, H., Ahmad, K.: Vibration analysis of a cantilevered beam with spring loading at the tip as a generic elastic structure. Appl. Mech. Mater. **629**, 407–413 (2014)
21. Musa, A.: Galerkin method for bending analysis of beams on non-homogeneous foundation. J. Appl. Math. Comput. Mech. **16**(3), 61–72 (2017)
22. Gunakala, S.R., Comissiong, D.M.G., Jordan, K., Sankar, A.: A finite element solution of the beam equation via MATLAB. KMUTNB. Int. J. Appl. Sci. Technol. **2**(8), 80–88 (2012)
23. Song, Z., Su, C.: Computation of Rayleigh damping coefficients for the seismic analysis of a hydro-powerhouse. Shock Vib. **2017**, 1–11 (2017)
24. Wang, Z., Li, L., Gong, M.: Measurement of dynamic modulus of elasticity and damping ratio of wood-based composites using the cantilever beam vibration technique. Constr. Build. Mater. **28**, 831–834 (2012)
25. Hujare, P., Sahasrabudhe, A.: Experimental investigation of damping performance of viscoelastic material using constrained layer damping treatment. Procedia Mater. Sci. **5**, 726–733 (2014)
26. Chandan, K., Patil, A.: Experimental modal frequency and damping estimation of viscoelastic material by circle fit method. Int. J. Curr. Eng. Technol. **6**(6), 2199–2204 (2016)
27. Brémaud, I.: Acoustical properties of wood in string instruments soundboards and tuned idiophones: biological and cultural diversity. J. Acoust. Soc. Am. **131**(1), 807–818 (2012)
28. Ross, J.: Wood handbook: wood as an engineering material. USDA Forest Service, Forest Products Laboratory, General Technical Report FPL- GTR-190, Forest Products Laboratory of U.S. Department of Agriculture (2010)
29. DeVisscher, J., Sol, H., DeWilde, W.: Identification of the damping properties of orthotropic composite materials using a mixed numerical experimental method. Appl. Compos. Mater. **4**(1), 13–33 (1997)
30. Faizah, R., Priyosulistyo, H., Aminullah, A.: An investigation on mechanical properties and damping behaviour of hardened mortar with rubber tire crumbs (RTC). In: MATEC Web of Conferences, vol. 258, pp. 1–6 (2019)